J Mater Sci (2009) 44:5980–5989
DOI 10.1007/s10853-009-3825-9

INTERFACE SCIENCE

Assigning physical significance to the diffuse interface between terraces in phase-field modeling of steps on crystal surfaces: modeling step–step interaction

Igal G. Rasin · Simon Brandon

Received: 9 June 2009 / Accepted: 19 August 2009 / Published online: 3 September 2009

Abstract We apply a modified phase-field modeling approach to the analysis of steps on a crystalline surface. Specifically, we are interested in capturing phenomena associated with the interaction between steps. To this end, we assign a physical significance to the form of the interfacial region between terraces (i.e. steps), inherent in the phase field approach, by tuning the multi-well potential to produce long-range interaction energies varying as $1/l^2$, where l is half the distance between steps. Resultant repulsive interactions between adjacent steps of the same sign are shown to affect step-flow kinetics in a manner consistent with curvature-driven interfacial relaxation. This phenomenon is further demonstrated to cause dislocation-driven (spiral) crystal growth kinetics to deviate, for large supersaturation and Burgers vector values, from the classical quadratic growth law. Attractive interactions between adjacent steps of opposite sign, also resulting from the finite interfacial width, are briefly explored particularly with respect to their possible impact on two-dimensional nucleation.

Introduction

The physics of advancing or receding crystalline surfaces involves phenomena spanning multiple spatial and temporal scales. Continuum modeling of such systems is limited to the analysis of relatively large time intervals and length scales. Short time-and-length scale physics, naturally modeled using a non-continuum approach (e.g. Monte Carlo or Molecular Dynamics), is typically accounted for in this case via the use of relevant transport and kinetic coefficients. One important small-scale physical phenomenon involves the entropic fluctuations of steps on crystalline surfaces, which are responsible for a form of step–step interaction that can be implemented in continuum models.

Although motivated by the need to include physics associated with step fluctuations in a continuum phase-field model of a crystalline surface, in this article we focus on all types of long-range effects (including fluctuations) whose contribution to the step energy is given by:

$$\gamma_{\text{int}} = b/l^2, \tag{1}$$

where l is the half terrace width and b is an interaction coefficient; relevant physics includes dipolar, elastic, and entropic interaction mechanisms. Dipolar step–step interactions (e.g. [1]) are a result of the formation of electric dipoles along steps, elastic interactions (e.g. [1–3]) are related to the overlap of strain fields associated with different steps, and entropic step–step interactions (e.g. [2]) are a result of entropic fluctuations of each step within the region defined by its nearest neighbors. In a real system it is often difficult to determine the relative contribution of each of these different mechanisms whose combined effect results in an overall interaction coefficient. A positive value of this coefficient (b), representing repulsive step–step interactions, is consistent with entropic and elastic (and sometimes dipolar) interactions between steps of the same sign (Fig. 1a). For the case of steps of opposite sign (Fig. 1b) b can be modeled as negative thereby rendering the interaction energy attractive in nature. This is relevant in certain cases of elastic interactions. In addition, entropic fluctuations are known to affect the annihilation of adjacent steps of opposite sign; it has been argued that this

I. G. Rasin · S. Brandon (✉)
Department of Chemical Engineering, Technion–Israel Institute of Technology, 32000 Haifa, Israel
e-mail: cersbsb@techunix.technion.ac.il

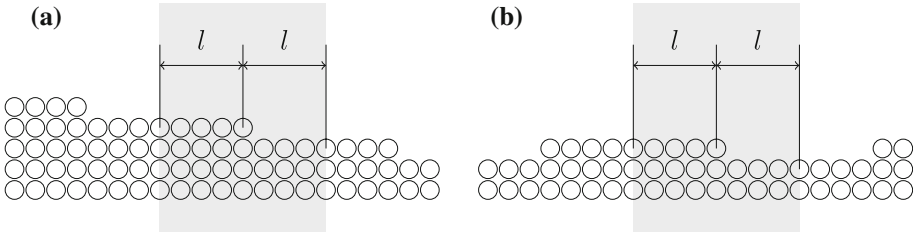

Fig. 1 Schematic illustration of steps on the surface. The *gray region* marks the domain of interest. **a** Steps of the same sign (in a step train). **b** Steps of opposite sign

phenomenon can be modeled as an effective attractive interaction [4]. Also, note that the observation in [5] that the time for annihilation is proportional to l^4 is consistent with the specific form of Eq. 1. Having said that, and following [4], we suggest that the $1/l^2$ attraction should be treated with caution as no more than a phenomenological rule which, as suggested below, could be modified in future applications.

Continuum modeling of vicinal surfaces is often based on the basic Burton-Cabrera-Frank (BCF) model [6], which originally involved the analysis of step flow while accounting for phenomena such as surface diffusion, step attachment kinetics, and the effect of energy associated with steps. Later versions of this approach involved the implementation of additional physical effects such as the Ehrlich–Schwoebel barrier and interaction with the bulk phase. The incorporation of step–step interaction of the type given by Eq. 1 within the framework of continuum modeling is typically limited to the case of one-dimensional (1-D) analyses of crystalline surfaces involving the explicit tracking of all steps in the system (see e.g. [7, 8]). Explicit tracking of steps can, however, be avoided by the application of the phase-field method when modeling such problems.

The phase-field method (see e.g. [9, 10]) is a powerful technique often applied in the investigation of crystal growth and solidification (see e.g. [11, 12]) as well as other systems exhibiting non-trivial evolution of microstructure (e.g. grain growth [13, 14]). An important feature of this approach, involving a diffuse interface approximation (whose position and thickness is determined by the spatial variation of an appropriate order parameter), is its ability to address topological changes in the system of interest without explicitly tracking the birth, evolution, and annihilation of interfaces between phases.

During the last decade and a half, the phase-field method was adapted for modeling the evolution of steps on a crystal surface (e.g. [15–19]). In these phase-field models, involving multi-well (in place of double-well) potentials, terraces (separated by diffuse steps) play the role of the different phases. Following the early study of Liu and Metiu [15] on the BCF model for step trains, more complex phenomena such as spiral growth [16], the Ehrlich–Schwoebel barrier [17–19], certain elastic effects [17, 20] as well as a combination of spiral growth with an additional non-trivial phenomenon [21, 22] were modeled using this type of approach.

In this article, we present a further development of the phase-field formulation for stepped crystalline surfaces, involving changes in the form of the multi-well potential. The resultant modification in the shape of the interface between neighboring terraces (i.e. steps) induces step–step interactions consistent with Eq. 1. The development of this approach and its application in a number of sample problems is discussed below.

Theory and computational details

Our approach is based on existing phase-field modeling techniques (see e.g. [19]) described in Eqs. 2–12 and henceforth referred to as "classical.". Using these classical methods, the value of the phase-field parameter (ϕ) can be related to the height of the crystal surface, above a reference plane, in units of single step-height (h_{st}). Integer values of the phase-field parameter correspond to the height of terraces while intermediate (non-integer) values of ϕ are associated with the vertical surface position within steps. It is convenient to describe the phase-field parameter, whose values are limited to the set of non-negative real numbers, as a sum of two parameters given by:

$$n(\phi) = \lfloor \phi \rfloor,\ \psi(\phi) = \phi - n(\phi), \tag{2}$$

where the first part of the equation involves the floor function [23] which, in this case, defines $n(\phi)$ as the highest integer less than or equal to ϕ; the remaining fractional part of ϕ is given by $\psi(\phi)$.

The spatio-temporal evolution of the phase-field parameter is derived by relating its local rate of change to the variation of the free-energy functional $\mathcal{F}$ describing the system and given, in our case, by the following volumetric integral:

$$\mathcal{F}(\phi) = \int_V \left(f(\phi) + \frac{\xi^2}{2} |\nabla \phi|^2 \right) \mathrm{d}V, \tag{3}$$

where $f(\phi)$ is the free-energy density function of a homogeneous system, the second term on the right-hand side (RHS) is associated with the step energy and ξ is its characteristic constant. The free-energy density is defined as a superposition of two terms:

$$f(\phi) = Wg(\phi) - \lambda p(\phi)\sigma, \tag{4}$$

where $g(\phi)$ is a multi-well potential [19] whose (zero valued) minima are associated with integer values of ϕ (i.e. $\phi = n$):

$$g(\phi) = \psi(\phi)^2[1 - \psi(\phi)]^2. \tag{5}$$

The second term on the RHS of Eq. 4, which corresponds to the reduction in energy due to solidification in a supersaturated environment, involves the level of supersaturation denoted by σ. In this article we assume negligible resistance to mass transport feeding the evolving steps; i.e. step flow is limited by kinetics of molecular attachment to the steps (see e.g. [24] for a review of crystal growth mechanisms). As a result of this assumption, the supersaturation on the surface is spatially uniform; we further limit it to be time-independent (i.e. σ = constant).

In Eq. 4 $p(\phi)$ (see e.g. [25]) is a monotonically increasing function which, on terraces ($\phi = n$), returns the value of the phase-field parameter (i.e. $p(n) = n$) and is thereby associated with the local number of solid layers above a reference plane. An appropriate choice for $p(\phi)$ is:

$$p(\phi) = 6\psi(\phi)^5 - 15\psi(\phi)^4 + 10\psi(\phi)^3 + n(\phi), \tag{6}$$

where, other than the above-mentioned ($p(n) = n$) condition, this fifth-order polynomial enforces zero first and second derivatives of $p(\phi)$ on terraces. Looking at Eqs. 4 and 5, it can be understood that the zero first derivative condition on $p(\phi)$ yields extrema in $f(\phi)$ at integer values of ϕ for any value of σ, and due to the zero second derivative condition these extrema are in fact stable minima (for further details see e.g. [26]).

The equation describing the spatio-temporal evolution of ϕ, corresponding to Eqs. 3 and 4 is given by [19]:

$$\tau\frac{\partial\phi}{\partial t} = \xi^2\Delta\phi - Wg'(\phi) + \lambda p'(\phi)\sigma, \tag{7}$$

where $g'(\phi)$ and $p'(\phi)$ are given by:

$$g'(\phi) = 2\psi(\phi)[1 - \psi(\phi)][1 - 2\psi(\phi)] \tag{8}$$

and

$$p'(\phi) = 30\psi(\phi)^4 - 60\psi(\phi)^3 + 30\psi(\phi)^2. \tag{9}$$

The step energy corresponding to this equation, for the case of straight steps, can be computed by the following integral in the direction orthogonal to the steps [27]:

$$\gamma_{st_0} = \int_{-\infty}^{\infty}\left[\frac{\xi^2}{2}|\nabla\phi|^2 + Wg(\phi)\right]dx = a_1\xi\sqrt{W}, \tag{10}$$

where

$$a_1 = \sqrt{2}\int_0^1\sqrt{g(\phi)}d\phi, \tag{11}$$

which, when using the classical $g(\phi)$ (given by Eq. 5), results in $a_1 = \frac{1}{3\sqrt{2}}$. The step energy is related to the Gibbs–Thomson coefficient according to $\Gamma_{st} = \gamma_{st_0}/\lambda$. In addition, the phase-field parameters ξ, W, λ, and τ are related to Γ_{st}, γ_{st_0}, the step kinetic coefficient β[1] and the width of transition region w via Eq. 10 as well as (e.g. [27]):

$$w = \frac{1}{a_1}\frac{\xi}{\sqrt{W}}, \quad \Gamma_{st} = a_1\frac{\xi\sqrt{W}}{\lambda}, \quad \beta = \frac{1}{a_1}\frac{\lambda\xi}{\tau\sqrt{W}}. \tag{12}$$

The classical solution can be used only for low step densities, $l \gg w$. For moderate to high values of step density, an interaction between adjacent steps (caused by the finite value of w) may impact the system's behavior. We next explore this artifact with the aim of using it to achieve physically meaningful step–step interactions.

Modifications to the classical approach

We start by proposing a new general form for the multi-well potential based on the influence of its shape on the above-mentioned interaction between steps. We note that $g(\phi)$ should have equal-valued minima for all cases where $\phi = n(\phi) = i$, $i = 0, 1,..., N$ while reaching a maximum value at some point in the range $i < \phi < i + 1$, $i = 0, 1,..., N - 1$ for every value of i in a system involving N steps (i.e. at some point on every step). In the classical case (corresponding to Eq. 5), the *local* shape of $g(\phi)$ near every minimum varies as a quadratic function of the deviation $\Delta\phi_i \equiv \phi - i$ where $i = 0, 1,..., N$ corresponds to the value of ϕ at the relevant minimum. As shown below, our goal of obtaining physically realistic long-range interaction between steps requires that we increase the order of the local dependence of $g(\phi)$ on $\Delta\phi_i$ near the minima.

Let us consider the following multi-well potential:

$$g(\phi) = \begin{cases} \psi(\phi)^\alpha, & \psi(\phi) < 1/2 \\ [1 - \psi(\phi)]^\alpha, & \psi(\phi) \geq 1/2 \end{cases}, \tag{13}$$

where α is an arbitrary parameter $\alpha > 2$, which directly defines the order of the local dependence of $g(\phi)$ on $\Delta\phi_i$ near every minimum and, as discussed above and shown below, governs the step–step interaction law.

Step–step interaction corresponding to the potential given by Eq. 13 is determined by calculating the dependence of step energy on the distance between steps. For this purpose, the 1-D domain $[-l, l]$, with a single step at its center, is considered. Approximate time-independent 1-D solutions of Eq. 7 for $\phi(x)$, corresponding to the stepped surfaces depicted in Fig. 1, are obtained for relatively large

[1] The product of the step kinetic coefficient (β) and the supersaturation (σ) is, for straight and non-interacting steps, the step velocity.

spacings between steps. Relevant boundary conditions are given by:

$$\phi(-l) = 1, \quad \phi(l) = 0, \tag{14}$$

for the case shown in Fig. 1a, and

$$\partial_x \phi|_{x=-l} = \partial_x \phi|_{x=l} = 0, \tag{15}$$

for the case shown in Fig. 1b. In the following, we summarize the results of our analysis of this problem; a more complete description is provided in Appendix 1.

The step energy is now described by the equation:

$$\gamma_{st} = \gamma_{st_0} + \gamma_{int}, \tag{16}$$

where γ_{st_0} is the energy for the case of $l \to \infty$ (given by Eq. 10) and γ_{int} is a step–step interaction energy. Our analysis shows that this interaction energy is positive (repulsive) in the case of Fig. 1a, is negative (attractive) in the case of Fig. 1b, and (in both cases) depends on the step–step distance according to:

$$\gamma_{int} = b_i / l^p, \quad p \equiv \frac{\alpha+2}{\alpha-2}, \tag{17}$$

where physically meaningful interactions correspond to $p > 0$. The interaction coefficient b_i is given by:

$$b_r = \left(4W^2 q_r^{-2\alpha} \xi^{-2\alpha}\right)^{\frac{1}{2-\alpha}} p^{-1}, \tag{18}$$

for the case of repulsive interactions (Fig. 1a) and by:

$$b_a = -\left(4W^2 q_a^{-2\alpha} \xi^{-2\alpha}\right)^{\frac{1}{2-\alpha}} p^{-1}, \tag{19}$$

for the case of attractive interactions (Fig. 1b). The parameters q_r and q_a, appearing in these equations, are given by:

$$q_r = \pi^{-1/2} \Gamma(1/2 - 1/\alpha) \Gamma(1 + 1/\alpha), \tag{20}$$

and

$$q_a = -\pi^{1/2} \Gamma(1/2 - 1/\alpha) / \Gamma(-1/\alpha), \tag{21}$$

where $\Gamma(z)$ is the Euler gamma function.[2] Finally, looking at Eqs. 18–21, it can be shown that the ratio of the interaction constants is fixed and depends only on α according to:

$$b_r / b_a = -\left(\sin\frac{\pi}{\alpha}\right)^{\frac{2\alpha}{2-\alpha}}. \tag{22}$$

It is interesting to note that the repulsive step–step interaction energy, important in step-trains, switches from being proportional to $1/l^p$ for large l values to being proportional to $1/l$ for small values of l. Specifically, the interaction energy for relatively large vicinalities (small l) is given by:

$$\gamma_{int} = \xi^2 / 4l, \tag{23}$$

a result which depends only on ξ and not on the shape of the multi-well potential.

Thus far, we have described a new multi-well potential $g(\phi)$. An appropriate choice for $p(\phi)$ should follow the same principles governing the selection of the form given by Eq. 6 in the case of the classical model. Using these principles, we choose a simple relation given by:

$$p(\phi) = \begin{cases} 0.5\left[\frac{\psi(\phi)}{0.5}\right]^{\alpha+1} + n(\phi), & \psi(\phi) < 1/2 \\ 1 - 0.5\left[\frac{1-\psi(\phi)}{0.5}\right]^{\alpha+1} + n(\phi), & \psi(\phi) \geq 1/2 \end{cases}. \tag{24}$$

As in the case of Eq. 6 in the classical approach, the modified $p(\phi)$ given by Eq. 24 is a monotonically increasing function which returns the value of the phase field parameter on terraces ($p(n) = n$) and guarantees the existence of stable minima in $f(\phi)$ (given by Eqs. 4 and 13) at integer values of ϕ for any value of σ. Note that applying Eq. 6, when using the new $g(\phi)$ given by Eq. 13, does not guarantee this behavior of $f(\phi)$ at integer values of ϕ.

Following the above derivation of Eq. 17, we propose the use of the potential given by Eq. 13 with $\alpha = 6$ as a method for simulating long-range interactions described by Eq. 1 (equivalent to Eq. 17 with $p = 2$). In this case, Eqs. 18–21 yield interaction coefficients given by:

$$b_r = \frac{0.975\xi^3}{\sqrt{W}}, \quad b_a = -\frac{0.122\xi^3}{\sqrt{W}}, \tag{25}$$

where, according to Eq. 22, $b_r/b_a = -8.0$. We do, however, realize the physically relevant necessity for the possibility of varying this ratio as a function of physical parameters and, although beyond the scope of this article, we speculate that it should be possible to achieve this via further adjustments in the definition of $g(\phi)$.

One of the main reasons we chose the specific form of $g(\phi)$ in Eq. 13 was that it enables the above analytical treatment leading to Eqs. 17–23. However, the rapid rise in $g(\phi)$ near the maxima in the potential ($\psi(\phi) = 0.5$) leads to significant grid-refinement requirements when attempting numerical analysis of Eq. 7. As stated above, we find that the main factor influencing step–step interaction is the behavior of $g(\phi)$ near its minima. We therefore replace Eq. 13, for $\psi_c < \psi(\phi) < 1 - \psi_c$ (i.e. far from the minima), by a simple constant valued interpolating function yielding (for this case of $\alpha = 6$):

$$g(\phi) = \begin{cases} \psi(\phi)^6, & \psi(\phi) \leq \psi_c \\ \psi_c^6, & \psi_c < \psi(\phi) < 1 - \psi_c \\ [1 - \psi(\phi)]^6, & \psi(\phi) \geq 1 - \psi_c \end{cases}. \tag{26}$$

We used $\psi_c = 0.35$, where further increase in the value of this parameter as well as using higher order interpolating

[2] Since $\alpha > 2$ both q_r and q_a are well defined positive numbers.

polynomials (see Appendix 2) did not significantly change our results; it is important to note that in this case (following Eq. 11), $a_1 = 0.0288013$. It is finally important to mention that in all calculations reported in this article the function $p(\phi)$, given in this case by Eq. 24 with $\alpha = 6$, did not cause numerical difficulties. Moreover, three alternative forms of $p(\phi)$ (see Appendix 2) were found to yield results almost identical to those obtained using Eq. 24.

In the next section, we present solutions of a number of problems, described by Eq. 7, using an explicit finite difference scheme. In all cases discussed here (1-D and 2-D), we employed a hyperbolic tangent phase-field parameter profile, centered around the initial position of the step, as an initial condition; results were found to be independent of the details of this initial shape. In addition, also in all cases discussed here, we employed a spatial discretization of $\delta_x = 0.125$ nm, a time step equal to $\delta_t = 0.0625$ μs, and physical parameters given by $h_{st} = 0.5$ nm, $\beta = 10^{-4}$ m/s, $\gamma_{st_0} = 10^{-11}$ J/m, $\Gamma_{st} = 0.47$ nm, $\eta_r = 0.3684$ nm, and $\eta_a = -0.1842$ nm, where $\eta_i \equiv \sqrt[3]{b_i/\lambda}$ $(i = r, a)$. Finally, note that periodic boundary conditions were applied in the 2-D simulations.

Results and discussion

We verify our approach using a 1-D simulation of the movement of a single step trapped, within a step train, between two adjacent (i.e. repulsing) steps under the condition of zero supersaturation. In this case, the computational domain $(0 < x < l_d)$ is comprised of two half-terraces on either side of the step. Relevant boundary conditions for Eq. 7 are given by:

$$\phi|_{x=0} = 1, \quad \phi|_{x=l_d} = 0, \tag{27}$$

and the initial step position, consistent with $\phi = 0.5$ and denoted by $x_{st} = x_0$, corresponds to a step–step spacing (terrace width) of $2x_0$ on the left and $2(l_d - x_0)$ on the right. A comparison between our numerical calculation and the integration of an analytical expression for the step velocity, given in [7] by:

$$v_{st} = \beta\eta_r^3\left(\frac{1}{x_{st}^3} - \frac{1}{(l_d - x_{st})^3}\right), \tag{28}$$

is presented in Fig. 2a. Since $x_0 < l_d/2$ the repulsive force from the left is larger than the one from the right resulting in the step moving to the right until it reaches the equilibrium position of $x_{st} = l_d/2$. Notice the high level of matching between the solutions considering the relatively coarse discretization ($l_d = 6.25$ nm $= 50\delta x$). In addition, note that the matching between the analytical and numerical solutions demonstrates how our use of an interpolating function for $g(\phi)$ far from the minima does not influence step–step interaction.

A second 1-D calculation explores the attractive force between steps in a configuration involving steps of alternating signs (i.e. a corrugated surface of the type shown in Fig. 1b) also under the condition of zero supersaturation. The boundary conditions for Eq. 7 are in this case:

$$\partial_x\phi|_{x=0} = \partial_x\phi|_{x=l_d} = 0, \tag{29}$$

where due to symmetry we need only solve for one of the steps. Initially, $\phi|_{x=0} = 1$ and $\phi|_{x=l_d} = 0$ and the step position is $x_{st} = x_0$ corresponding to interstep spacings of $2x_0$ on the left and $2(l_d - x_0)$ on the right. The analytical solution for the step velocity is in this case also given by Eq. 28 though with η_a replacing η_r. The time-dependent position of the step is plotted in Fig. 2b. According to the initial condition $(x_0 < l_d/2)$, the step is more strongly attracted to the left and therefore accelerates in this direction toward its ultimate annihilation ($x_{st} = 0$). As in the previous test a good agreement between numerical computations and theory is observed.

The classical theory of spiral growth, which is based on analysis of processes in the vicinity of a dislocation core, predicts [6] a quadratic dependence of crystal growth rate on supersaturation. However, this theory assumes a constant value for the step energy. It is therefore reasonable to believe that, when the step density near the dislocation core is large enough, step–step interactions may cause a deviation from the classical growth law. As is evident from our 2-D simulations (Fig. 3) a deviation from the classical law

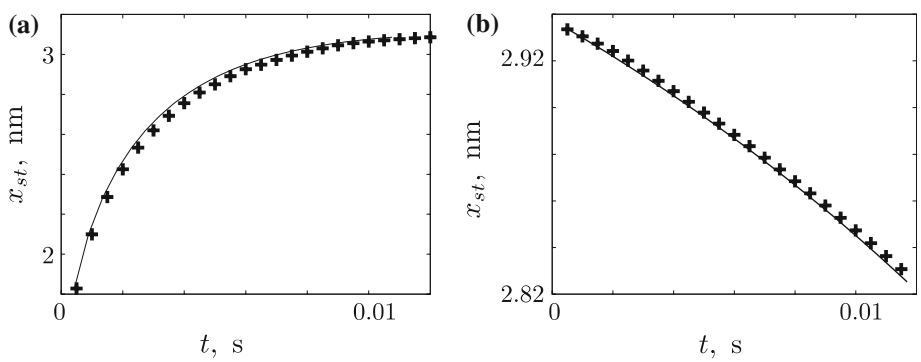

Fig. 2 Step position versus time. *Symbols* correspond to numerical results and the *solid line* to the analytical solution. The domain size is given by $l_d = 6.25$ nm. **a** Repulsion in a step train, $x_0 = 1.313$ nm. **b** Attraction in a corrugated surface, $x_0 = 2.938$ nm

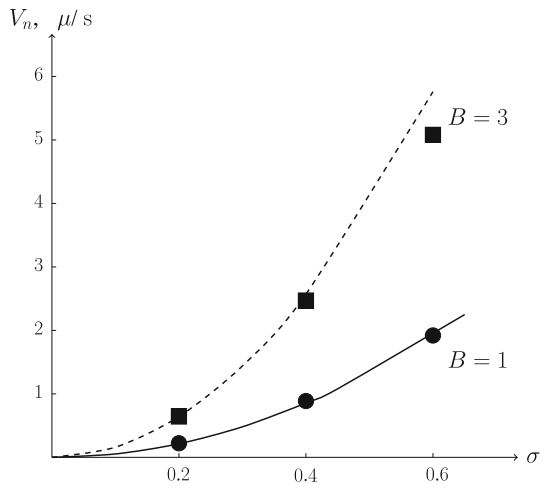

Fig. 3 Spiral growth rate versus supersaturation for two different values of the Burgers vector: $B = 1$ (*solid line* and *filled circle symbols*) and $B = 3$ (*dashed line* and *filled square symbols*). *Lines* correspond to the classical spiral growth law $V_n = \beta\, h_{st}\sigma^2/(19\Gamma_{st})$ and *symbols* are due to our simulations. The domain size is 25×25 nm^2

is seen for relatively large supersaturation (σ) and Burgers vector (B) values. Indeed the step density does increase with an increase in the value of these two parameters. Considering the fact that using alternative forms of $p(\phi)$ (see Appendix 2) does not significantly change this result suggests that this deviation from the classical theory is dominated by the form of $g(\phi)$. Finally, it is interesting to note that the resultant retardation of crystal growth stands in contrast to the acceleration of growth expected when 2-D nucleation of new layers occurs on the surface (see e.g. [28]).

We next consider two adjacent circular *nominally* super-critical nuclei and compare their behavior to that of a single nucleus; both these cases are contrasted with that of a single nucleus calculated with the classical model (with $g(\phi)$ given by Eq. 5 and $p(\phi)$ given by Eq. 6) using the same physical parameters and with a transition region width (see Eq. 12) given by $w = 0.75$ nm. The initial radius of each nucleus, the level of supersaturation, and the initial distance between the centers of the two neighboring nuclei are, respectively, $r_0 = 2.0$ nm, $\sigma = 0.239$, and $d = 8$ nm. As expected (Fig. 4a), the isolated nucleus modeled using the classical approach grows with time since its initial radius is larger than the calculated critical value ($r_{c_0} = \Gamma_{st}/\sigma = 1.97$ nm). As shown in Fig. 4b, it is surprising to observe the shrinking of the isolated nucleus, modeled with our modified phase-field model, whose initial radius is (as in the case shown in Fig. 4a) also larger than the classical critical value. This observation can be explained when considering that, due to self-attraction of the circular step, the true critical radius value is actually larger than r_{c_0} and, in this case, even larger than r_0. Increasing r_0 will eventually lead to a truly super-critical nucleus which will grow with time.

In contrast to the shrinking single nucleus, it is interesting to observe (Fig. 4c) the growth and coalescence of

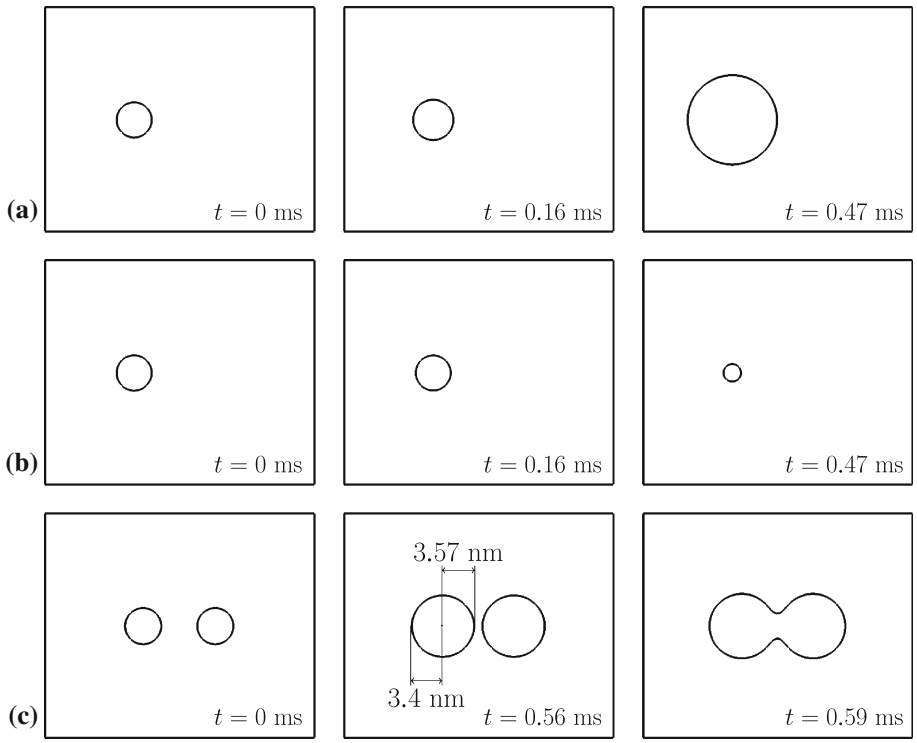

Fig. 4 Evolution of 2-D nuclei. **a** Isolated nucleus calculated with classical model ($g(\phi)$ and $p(\phi)$, respectively, given by Eqs. 5 and 6). **b** Isolated nucleus calculated with modified model ($g(\phi)$ and $p(\phi)$, respectively, given by Eqs. 13 and 24 with $\alpha = 6$). **c** Two adjacent nuclei calculated with modified model ($g(\phi)$ and $p(\phi)$, respectively, given by Eqs. 13 and 24 with $\alpha = 6$); notice the non-circular (asymmetric) shape of the adjacent nuclei as they become close one to the other. Domain size is 30×25 nm^2

two adjacent nuclei. The attractive interaction between the two particles acts in favor of their growth, despite the fact (discussed above) that isolated particles of the same initial size ($r_0 = 2.0$ nm) are effectively sub-critical. As in the case of spiral growth, using alternative forms of $p(\phi)$ (see Appendix 2) does not significantly change these results, thereby indicating that the observed deviation from classical theory is primarily a result of the chosen form of $g(\phi)$. Finally, it should be noted that these results demonstrate the possible non-trivial impact of attractive interactions, within and between nuclei, on 2-D nucleation processes.

Conclusions

We have assigned a physical significance to the form of the terrace–terrace interfacial region inherent in phase-field modeling of steps on a crystal surface. Specifically, the multi-well potential $g(\phi)$ was modified to obtain a (low-step density) step–step interaction energy proportional to $1/l^p$, repulsive for steps of the same sign and attractive for steps of opposite sign. We investigated the physically relevant case of $p = 2$, first verifying the algorithm via 1-D simulations, next demonstrating the retardation of spiral growth due to repulsive interactions at high B and σ values and finally presenting evidence for non-trivial impact of attractive interactions on 2-D nucleation phenomena.

In this article, we have taken σ to be constant. This assumption could however be relaxed, e.g. in the case of crystal growth from solution with significant resistance to mass transport of the solute feeding the evolving steps (e.g. [29]). In such a case, Eq. 7 should be coupled with an additional partial differential equation describing the transport of the nutrient to the steps. This is similar in spirit to the approach used in the phase-field model of epitaxy described in [19].

Theories for step–step interactions are usually based on the analysis of straight steps. Although we tuned our model to agree with the $1/l^2$ law for straight steps at relatively large distances, the 2-D simulations inherently include the effect of curvature which does require further analysis. In addition, we speculate that the fixed nature of b_r/b_a as well as the $1/l^2$ rule for attractive interactions may possibly be modified (without changing the nature of repulsive interactions) by further adjustments to $g(\phi)$. Finally, we suggest that the general nature of our approach (involving modifications in $g(\phi)$ and associated adjustments to $p(\phi)$) should make it applicable to a wide range of problems. These may involve interactions between surfaces of 3-D solid particles as well as those existing in nano-scale liquid systems (see e.g. [30, 31]).

Acknowledgements The authors thank Dr. A. Virozub for his mathematical insight related to this article. This research was supported by THE ISRAEL SCIENCE FOUNDATION (Grant No. 1190/04).

Appendix 1: derivation of step–step interaction parameters

In this appendix we provide details of the analytical treatment leading to the derivation of Eqs. 17–23. We first start with the derivation of the case of repulsing steps in a step train, consistent with Fig. 1a and described by the stationary 1-D solution of Eq. 7 in the spatial interval $[-l, l]$ with boundary conditions given by Eq. 14. Our goal is to demonstrate how our choice of $g(\phi)$, given by Eq. 13, leads to the desired power law dependence of step–step interaction energy on the distance between steps. Moreover, we wish to find the relation between the parameters of the interaction law and those appearing in Eqs. 7 (τ, ξ, W, λ) and 13 (α).

The stationary 1-D version of Eq. 7, with the assumption of relatively low supersaturation values ($\lambda\sigma \ll W$ and $\lambda\sigma \ll \xi^2$) is given by:

$$\xi^2 \frac{\mathrm{d}^2\phi}{\mathrm{d}x^2} - Wg'(\phi) = 0. \tag{30}$$

This equation can be re-written and integrated according to:

$$\xi^2 \int \frac{\mathrm{d}\phi}{\mathrm{d}x} d\left(\frac{\mathrm{d}\phi}{\mathrm{d}x}\right) = W \int \mathrm{d}g(\phi), \tag{31}$$

which, while remembering that $g(\phi(l)) = 0$, yields:

$$\frac{\xi^2}{2}\left(\frac{\mathrm{d}\phi}{\mathrm{d}x}\right)^2 = Wg(\phi) + \frac{\xi^2}{2}G_r, \tag{32}$$

where $G_r \equiv \left(\frac{\mathrm{d}\phi}{\mathrm{d}x}|_{x=l}\right)^2$.

Taking the square root of both sides of Eq. 32, while remembering that in this case $\frac{\mathrm{d}\phi}{\mathrm{d}x} < 0$, rearranging the results and integrating between $x = 0$ ($\phi = 1/2$) and $x = l$ ($\phi = 0$) yields:

$$\begin{aligned} l &= \xi \int_0^{1/2} \frac{\mathrm{d}\phi}{\sqrt{2Wg(\phi) + \xi^2 G_r}} \\ &= \xi \int_0^{\infty} \frac{\mathrm{d}\phi}{\sqrt{2W\tilde{g}(\phi) + \xi^2 G_r}} - \xi \int_{1/2}^{\infty} \frac{\mathrm{d}\phi}{\sqrt{2W\tilde{g}(\phi) + \xi^2 G_r}}, \end{aligned} \tag{33}$$

where $\tilde{g}(\phi) \equiv \phi^\alpha$. Assuming a relatively large distance between steps ($G_r \ll 2W/(2^\alpha \xi^2)$) we now obtain:

$$l = \xi \int_0^{\infty} \frac{\mathrm{d}\phi}{\sqrt{2W\phi^{\alpha} + \xi^2 G_r}} - \xi \int_{1/2}^{\infty} \frac{\mathrm{d}\phi}{\sqrt{2W\phi^{\alpha}}}$$
$$= \frac{q_r}{\sqrt{G_r}} \left(\frac{\xi^2 G_r}{2W}\right)^{1/\alpha} - \frac{2^{\frac{\alpha-1}{2}}}{\alpha - 2} \frac{\xi}{\sqrt{W}}, \quad (34)$$

where q_r is defined in Eq. 20.

The step energy is now calculated using the equation:

$$\gamma_{\mathrm{st}} = \int_{-l}^{l} \left[\frac{\xi^2}{2}\left(\frac{\mathrm{d}\phi}{\mathrm{d}x}\right)^2 + Wg(\phi)\right] \mathrm{d}x. \quad (35)$$

This equation is next re-written, with the help of Eq. 32 while remembering that $\frac{\mathrm{d}\phi}{\mathrm{d}x} < 0$, to yield:

$$\gamma_{\mathrm{st}} = \int_{-l}^{l} \left[\xi^2 \left(\frac{\mathrm{d}\phi}{\mathrm{d}x}\right)^2 - \frac{\xi^2}{2} G_r\right] \mathrm{d}x$$
$$= \xi \int_{l}^{-l} \sqrt{2Wg(\phi) + \xi^2 G_r} \frac{\mathrm{d}\phi}{\mathrm{d}x} \mathrm{d}x - \xi^2 G_r l$$
$$= \xi \int_0^1 \sqrt{2Wg(\phi) + \xi^2 G_r} \mathrm{d}\phi - \xi^2 G_r l. \quad (36)$$

We next compare the first term of this result with Eq. 33, while accounting for symmetry with respect to $\phi = 0.5$ and remembering our assumption of a relatively large distance between steps. It can be seen this term is proportional to the integral of Eq. 33 with respect to G_r. With this information, together with Eq. 34, we can see that:

$$\gamma_{\mathrm{st}} = 2\xi \int_0^{1/2} \sqrt{2Wg(\phi) + \xi^2 G_r} \mathrm{d}\phi - \xi^2 G_r l$$
$$= \xi^2 \int_0^{G_r} l(G_r^*) \mathrm{d}G_r^* - \xi^2 G_r l + \gamma_{\mathrm{st}_0}$$
$$= \xi^2 \int_0^{G_r} \frac{q_r}{\sqrt{G_r^*}} \left(\frac{\xi^2 G_r^*}{2W}\right)^{1/\alpha} \mathrm{d}G_r^* - \frac{2^{\frac{\alpha-1}{2}}}{\alpha - 2} \frac{\xi^3}{\sqrt{W}} G_r$$
$$- \xi^2 G_r l + \gamma_{\mathrm{st}_0}, \quad (37)$$

where γ_{st_0} is the constant of integration (with respect to G_r) which corresponds to the value of the step energy in the limit of $l \to \infty$ ($G_r \to 0$) in which case step–step interactions disappear. Equation 37 is further simplified (with the aid of Eq. 34 to yield:

$$\gamma_{\mathrm{st}} = \frac{2\alpha}{2 + \alpha} \xi^2 G_r \left(l + \frac{2^{\frac{\alpha-1}{2}}}{\alpha - 2} \frac{\xi}{\sqrt{W}}\right) - \frac{2^{\frac{\alpha-1}{2}}}{\alpha - 2} \frac{\xi^3}{\sqrt{W}} G_r$$
$$- \xi^2 G_r l + \gamma_{\mathrm{st}_0}. \quad (38)$$

Remembering (see Eq. 16) that $\gamma_{\mathrm{int}} = \gamma_{\mathrm{st}} - \gamma_{\mathrm{st}_0}$ and inserting the dependence of G_r on l (extracted from Eq. 34) into Eq. 38 yields the following expression for the step–step interaction energy:

$$\gamma_{\mathrm{int}} = \left(\frac{\alpha - 2}{\alpha + 2}\right) \xi^2 \left(l + \frac{2^{\frac{\alpha-1}{2}}}{\alpha - 2} \frac{\xi}{\sqrt{W}}\right) G_r$$
$$= \left(\frac{\alpha - 2}{\alpha + 2}\right) \left[\frac{2W}{(\xi q_r)^{\alpha}}\right]^{\frac{2}{2-\alpha}} \left(l + \frac{2^{\frac{\alpha-1}{2}}}{\alpha - 2} \frac{\xi}{\sqrt{W}}\right)^{\frac{2+\alpha}{2-\alpha}}$$
$$= b_r \left(l + \frac{2^{\frac{\alpha-1}{2}}}{\alpha - 2} \frac{\xi}{\sqrt{W}}\right)^{\frac{2+\alpha}{2-\alpha}}, \quad (39)$$

where b_r is given by Eq. 18. Remembering the above assumption of relatively large distance between steps ($G_r \ll 2W/(2^{\alpha}\xi^2)$), we can see that for $l \gg \frac{2^{\frac{\alpha-1}{2}}}{\alpha-2} \frac{\xi}{\sqrt{W}}$ we obtain, from Eq. 39, the power law given by Eq. 17.

We next return to Eq. 33 and consider now the case of short distances between steps ($G_r \gg 2W/(2^{\alpha}\xi^2)$). With this assumption it is easy to show that

$$l = (4G_r)^{-1/2}, \quad (40)$$

and following Eq. 36 one can show (with the above short step–step distance assumption) that:

$$\gamma_{\mathrm{st}} = \xi^2 \left(\sqrt{G_r} - G_r l\right), \quad (41)$$

and, after inserting $G_r(l)$ from Eq. 40 into Eq. 41 we obtain:

$$\gamma_{\mathrm{st}} = \xi^2 \left[1/(2l) - l/(4l^2)\right] = 0.25\xi^2/l. \quad (42)$$

Now $G_r \gg 2W/(2^{\alpha}\xi^2) \geq 2Wg(\phi)/\xi^2$ (for all values of ϕ), and as a result $\xi^2\sqrt{G_r} \gg \xi\sqrt{2Wg(\phi)}$ (for all values of ϕ). Therefore, $\int_0^{1/2} \xi^2\sqrt{G_r}\mathrm{d}\phi \gg \int_0^{1/2} \xi\sqrt{2Wg(\phi)}\mathrm{d}\phi$ and, due to symmetry with respect to $\phi = 0.5$, $\xi^2\sqrt{G_r} \gg \left(\sqrt{2}\int_0^1 \sqrt{g(\phi)}\mathrm{d}\phi\right)\xi\sqrt{W}$. Comparing with Eqs. 10 and 11, we see that we have obtained $\xi^2\sqrt{G_r} \gg \gamma_{\mathrm{st}_0}$. Using $G_r(l)$ from Eq. 40 we further understand that $\xi^2/(2l) \gg \gamma_{\mathrm{st}_0}$ and, with the aid of Eq. 42, it is reasonable to conclude that $\gamma_{\mathrm{st}} \gg \gamma_{\mathrm{st}_0}$ which means that the step energy is dominated by step–step interactions and Eq. 42 is equivalent to Eq. 23.

Finally, we address the case of attracting steps, consistent with Fig. 1b and described by the stationary 1-D solution of Eq. 7 in the spatial interval $[-l,l]$ with boundary conditions given by Eq. 15. Our starting point is Eq. 30 which, when remembering $\frac{\mathrm{d}\phi}{\mathrm{d}x}|_{x=l} = 0$ yields:

$$\frac{\xi^2}{2}\left(\frac{\mathrm{d}\phi}{\mathrm{d}x}\right)^2 = Wg(\phi) - WG_a, \tag{43}$$

where $G_a \equiv g(\phi(x))|_{x=l}$. Following the same approach used in the derivation of Eqs. 33 and 34 we next isolate l under the assumption that $G_a \ll \frac{1}{2^\alpha}$ while understanding that $\frac{\mathrm{d}\phi}{\mathrm{d}x} < 0$, $x = 0$ corresponds to $\phi = 1/2$ and $x = l$ corresponds to $\phi(l) = G_a^{1/\alpha}$. The result is given by:

$$\begin{aligned} l &= \xi \int_{G_a^{1/\alpha}}^{1/2} \frac{\mathrm{d}\phi}{\sqrt{2W(\phi^\alpha - G_a)}} \\ &= \xi \int_{G_a^{1/\alpha}}^{\infty} \frac{\mathrm{d}\phi}{\sqrt{2W(\phi^\alpha - G_a)}} - \xi \int_{1/2}^{\infty} \frac{\mathrm{d}\phi}{\sqrt{2W\phi^\alpha}} \\ &= \frac{\xi q_a}{\sqrt{2W}} G_a^{\frac{2-\alpha}{2\alpha}} - \frac{2^{\frac{\alpha-1}{2}}}{\alpha - 2}\frac{\xi}{\sqrt{W}}, \end{aligned} \tag{44}$$

where q_a is defined in Eq. 21.

We next start with the definition of the step energy given by Eq. 35 and following the same logic as in the case of step–step repulsion, with the aid of Eq. 43, we can show that:

$$\begin{aligned} \gamma_{\mathrm{st}} &= \int_{-l}^{l} \left[\xi^2\left(\frac{\mathrm{d}\phi}{\mathrm{d}x}\right)^2 + WG_a\right]\mathrm{d}x \\ &= \xi \int_{l}^{-l} \sqrt{2W[g(\phi) - G_a]}\frac{\mathrm{d}\phi}{\mathrm{d}x}\mathrm{d}x + 2WG_a l \\ &= 2\xi \int_{G_a^{1/\alpha}}^{1/2} \sqrt{2W[g(\phi) - G_a]}\mathrm{d}\phi + 2WG_a l, \end{aligned} \tag{45}$$

which is further simplified to become:

$$\begin{aligned} \gamma_{\mathrm{st}} &= -2W \int_0^{G_a} l(G_a^*)\mathrm{d}G_a^* + 2WG_a l + \gamma_{\mathrm{st}_0} \\ &= -2W \int_0^{G_a} \frac{\xi q_a}{\sqrt{2W}} G_a^{*\frac{2-\alpha}{2\alpha}}\mathrm{d}G_a^* + \frac{2^{\frac{\alpha+1}{2}}}{\alpha - 2}\xi\sqrt{W}G_a \\ &\quad + 2WG_a l + \gamma_{\mathrm{st}_0} \\ &= -\frac{2\alpha}{2+\alpha}\xi q_a\sqrt{2W}G_a^{\frac{2+\alpha}{2\alpha}} + \frac{2^{\frac{\alpha+1}{2}}}{\alpha - 2}\xi\sqrt{W}G_a \\ &\quad + 2WG_a l + \gamma_{\mathrm{st}_0}. \end{aligned} \tag{46}$$

Inserting $G_a(l)$ from Eq. 44 and recalling Eq. 16, we obtain the interaction energy:

$$\begin{aligned} \gamma_{\mathrm{int}} &= \left(\frac{2-\alpha}{\alpha+2}\right)\left[\frac{2W}{(\xi q_a)^\alpha}\right]^{\frac{2}{2-\alpha}}\left(l + \frac{2^{\frac{\alpha-1}{2}}}{\alpha - 2}\frac{\xi}{\sqrt{W}}\right)^{\frac{2+\alpha}{2-\alpha}} \\ &= b_a\left(l + \frac{2^{\frac{\alpha-1}{2}}}{\alpha - 2}\frac{\xi}{\sqrt{W}}\right)^{\frac{2+\alpha}{2-\alpha}}, \end{aligned} \tag{47}$$

where b_a is given by Eq. 19. Here, as in the case of repulsion, the assumption of large step–step distances ($G_a \ll \frac{1}{2^\alpha}, l \gg \frac{2^{\frac{\alpha-1}{2}}}{\alpha-2}\frac{\xi}{\sqrt{W}}$) renders Eq. 47 equivalent to the power law given by Eq. 17.

Appendix 2: testing alternative forms of $g(\phi)$ and $p(\phi)$

In the text we discuss the replacement of Eq. 13, for $\psi_c < \psi(\phi) < 1 - \psi_c$, by a simple constant valued interpolating function yielding $g(\phi)$ given by Eq. 26. In addition to varying the value of ψ_c (mentioned in the text), we tested the sensitivity of the model to this interpolating function using a more general alternative to Eq. 26 given by:

$$g(\phi) = \begin{cases} \psi(\phi)^6, & \psi(\phi) \le \psi_c \\ \Sigma_{i=0}^{m} c_i \psi(\phi)^i [1 - \psi(\phi)]^i, & \psi_c < \psi(\phi) < 1 - \psi_c \\ [1 - \psi(\phi)]^6, & \psi(\phi) \ge 1 - \psi_c \end{cases}, \tag{48}$$

with c_i determined by enforcing continuity in $g(\phi)$ and its derivatives (up to order m) at ψ_c and $1 - \psi_c$. For a given level of supersaturation, and physical parameter values, results with $m = 0$ (in which case Eq. 48 is equivalent to Eq. 26) were found to be virtually the same as those achieved with $m = 3$.

Results presented in Figs. 3 and 4 were reproduced using three alternative forms for $p(\phi)$, all of which are monotonically increasing functions which return the value of the phase-field parameter on terraces ($p(n) = n$) and guarantee the existence of stable minima in $f(\phi)$ (given by Eqs. 4 and 13) at integer values of ϕ for any value of σ. In the first case, Eq. 24 (with $\alpha = 6$) was modified using a linear interpolation in the region $\psi_c < \psi(\phi) < 1 - \psi_c$, yielding:

$$p(\phi) = \begin{cases} 0.5\left[\frac{\psi(\phi)}{0.5}\right]^7 + n(\phi), & \psi(\phi) \le \psi_c \\ 0.5\left(\frac{\psi_c}{0.5}\right)^7 + n(\phi) + \frac{[\psi(\phi) - \psi_c]}{2(1-2\psi_c)} & \\ \quad \times\left[2 - \left(\frac{1-\psi_c}{0.5}\right)^7 - \left(\frac{\psi_c}{0.5}\right)^7\right], & \psi_c < \psi(\phi) < 1 - \psi_c \\ 1 - 0.5\left[\frac{1-\psi(\phi)}{0.5}\right]^7 + n(\phi), & \psi(\phi) \ge 1 - \psi_c \end{cases}. \tag{49}$$

The second case, given by:

$$p(\phi) = \begin{cases} 0.25\left[\frac{\psi(\phi)}{0.5}\right]^7 + n(\phi), & \psi(\phi) \le \psi_c \\ 0.25\left(\frac{\psi_c}{0.5}\right)^7 + n(\phi) + \frac{[\psi(\phi) - \psi_c]}{4(1-2\psi_c)} & \\ \quad \times\left[4 - \left(\frac{1-\psi_c}{0.5}\right)^7 - \left(\frac{\psi_c}{0.5}\right)^7\right], & \psi_c < \psi(\phi) < 1 - \psi_c \\ 1 - 0.25\left[\frac{1-\psi(\phi)}{0.5}\right]^7 + n(\phi), & \psi(\phi) \ge 1 - \psi_c \end{cases}, \tag{50}$$

is similar in form to Eq. 49 except for the fact that the power law terms are pre-multiplied by a factor of 0.25 rather than by a factor of 0.5. Note that in Eq. 24 the factor of 0.5 is necessary for continuity at $\phi = 0.5$ (where $p(0.5) = 0.5$). Notice also that the specific forms of the linear part of $p(\phi)$ in Eqs. 49 and 50 (in the region $\psi_c < \psi(\phi) < 1 - \psi_c$) guarantees continuity of this function for all values of ϕ (where here too $p(0.5) = 0.5$).

The last alternative form of $p(\phi)$ is given by

$$p(\phi) = \begin{cases} 0.5\left[\frac{\psi(\phi)}{0.5}\right]^8 + n(\phi), & \psi(\phi) < 1/2 \\ 1 - 0.5\left[\frac{1-\psi(\phi)}{0.5}\right]^8 + n(\phi), & \psi(\phi) \geq 1/2 \end{cases}, \quad (51)$$

where in this case the exponent of the power law was increased. Repeating calculations for the cases involving a non-zero value of supersaturation (presented in Figs. 3 and 4), using all three alternative forms of $p(\phi)$ (Eqs. 49–51 with $\psi_c = 0.35$), yielded results virtually the same as those obtained using Eq. 24.

References

1. Jayaprakash C, Rottman C, Saam WF (1984) Phys Rev B 30:6549
2. Pimpinelli A, Villain J (1998) Physics of crystal growth. Cambridge University Press, Cambridge
3. Müller P, Saúl A (2004) Surf Sci Rep 54:157
4. Israeli N, Kandel D (2000) Phys Rev B 62(20):13707
5. Selke W, Duxbury PM (1995) Phys Rev B 52(24):17468
6. Burton WK, Cabrera N, Frank FC (1951) Philos Trans R Soc A 243:299
7. Fu ES, Johnson MD, Liu D-J, Weeks JD, Williams ED (1996) Phys Rev Lett 77(6):1091
8. Dai B (2005) PhD thesis, The Graduate School of the University of Minnesota
9. Karma A (2005) In: Yip S (ed) Handbook of materials modeling. Part B. Springer, Dordrecht
10. Emmerich H (2008) Adv Phys 57(1):1
11. Kim SG, Kim WT (2005) In: Yip S (ed) Handbook of materials modeling. Part B. Springer, Dordrecht
12. Tang J, Xue X (2009) J Mater Sci 44:745. doi:10.1007/s10853-008-3157-1
13. Krill KE III (2005) In: Yip S (ed) Handbook of materials modeling. Part B. Springer, Dordrecht
14. McKenna IM, Gururajan MP, Voorhees PW (2009) J Mater Sci 44:2206. doi:10.1007/s10853-008-3196-7
15. Liu F, Metiu H (1994) Phys Rev E 49(4):2601
16. Karma A, Plapp M (1998) Phys Rev Lett 81(20):4444
17. Emmerich H (2003) Continuum Mech Thermodyn 15(2):197
18. Pierre-Louis O (2003) Phys Rev E 68(2):021604
19. Rätz A, Voigt A (2004) J Cryst Growth 266:278
20. Yeon D-H, Cha P-R, Chung S-I, Yoon J-K (2004) Met Mater Int 9(1):67
21. Redinger A, Ricken O, Kuhn P, Rätz A, Voigt A, Krug J, Michely T (2009) Phys Rev Lett 100:035506
22. Yu Y-M, Liu B-G, Voigt A (2009) Phys Rev B 79(23):235317
23. Graham R, Knuth D, Patashnik O (1994) Concrete mathematics: a foundation for computer science, 2 edn. Addison-Wesley, Reading
24. van der Erden JP (1993) In: Hurle DTJ (ed) Handbook of crystal growth, vol 1a: bulk fundamentals, growth thermodynamics and kinetics. North-Holland, Amsterdam
25. Provatas N, Greenwood M, Athreya B, Goldenfeld N, Dantzig J (2005) Int J Mod Phys B 19(31):4525
26. Wang S-L, Sekerka RF, Wheeler AA, Murray BT, Coriell SR, Brown RJ, McFadden GB (1993) Physica D 69:189
27. Karma A, Rappel W-J (1998) Phys Rev E 57(4):4323
28. Bennema P, Kern R, Simon B (1967) Phys Status Solidi 19(1):211
29. Kwon Y-I, Dai B, Derby JJ (2007) Prog Cryst Growth Charact Mater 53:167
30. Moseler M, Landman U (2000) Science 289(5482):1165
31. Kang W, Landman U (2007) Phys Rev Lett 98(6):064504/1